

# Size effect on surface structural relaxation kinetics of silica glass sample

A. Koike, M. Tomozawa \*

*Department of Materials Science and Engineering, Rensselaer Polytechnic Institute, School of Engineering,  
110 8th Street, Troy, NY 12180-3590, USA*

Received 22 December 2005; received in revised form 2 June 2006  
Available online 23 August 2006

## Abstract

It is known that surface structural relaxation takes place more rapidly than bulk structural relaxation, especially in the presence of water vapor. The surface structural relaxation kinetics of the silica glass fiber and plates was compared at 950 °C and the surface structural relaxation kinetics of silica glass fiber was found to be faster than that of the silica glass plate, even though the composition and initial fictive temperatures of the samples were the same. The observed difference of the surface structural relaxation kinetics between silica glass fiber and silica glass plate can be accounted for using a diffusion equation with time-dependent surface concentration. The analysis indicates that there is a general size effect on the surface structural relaxation kinetics, with smaller sized samples exhibiting faster relaxation kinetics.

© 2006 Elsevier B.V. All rights reserved.

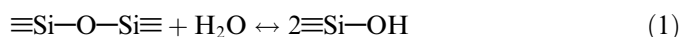
PACS: 61.43.Fs; 64.70.Pf; 65.80.+n; 78.30.-j

Keywords: Glasses; FTIR measurements; Oxide glasses; Silica; Surfaces and interfaces; Structural relaxation; Water in glass

## 1. Introduction

The properties of a glass at room temperature, in general, are influenced by its thermal history. This phenomenon is attributed to a different fictive temperature of the glass [1]. When a glass is heated at a constant temperature near its glass transition temperature, its fictive temperature approaches the heating temperature due to structural relaxation. Our previous studies [2–4] showed that structural relaxation kinetics of silica glass was different for the glass surface and bulk. The surface structural relaxation takes place more rapidly than the bulk structural relaxation, especially in the presence of water vapor. Water can diffuse into a silica glass when the glass is heat-treated in the presence of water vapor. Diffusion of water into glasses takes place through the diffusion of molecular water (H<sub>2</sub>O) and

its reaction with the glass structure to form immobile hydroxyl (–OH) [5] as shown below.



This reaction is believed to reach its equilibrium quickly at a high temperature, with the hydroxyl being the dominant water species. Water content in glass can be determined using infrared (IR) spectroscopy: hydroxyl content in silica glasses can be determined by measuring the absorbance at the  $\sim 3670 \text{ cm}^{-1}$  band, while molecular water content can be determined by measuring absorbance at the  $\sim 3400 \text{ cm}^{-1}$  band [6–8]. However, most commercial silica glasses exhibit only the hydroxyl band. The hydroxyl concentration profiles in silica glasses change with the hydration heat-treatment but this is not the result of the direct motion of hydroxyl but the result of the diffusion of molecular water and its reaction with the glass by Eq. (1).

By using the IR water-related bands and silica structural bands, Davis and Tomozawa [9] investigated the relation

\* Corresponding author. Tel.: +518 276 6451; fax: +518 276 8554.  
E-mail address: [tomozm@rpi.edu](mailto:tomozm@rpi.edu) (M. Tomozawa).

between kinetics of structural relaxation and water diffusion of a silica glass in wide range of temperatures. They found that both the depth of hydroxyl water formation and the depth of the relaxed surface layer increased with time by diffusion-controlled processes and obtained the effective diffusion coefficients of surface structural relaxation and hydroxyl water diffusion, separately. At temperatures higher than 850 °C, effective diffusion coefficient of surface structural relaxation was higher than that of hydroxyl. For example, for a silica glass heated at 1000 °C for 4 h in 355 Torr water vapor pressure, surface structural relaxation reached around 500  $\mu\text{m}$  from the surface, while hydroxyl reached only around 60  $\mu\text{m}$  [4]. From these observations, it was suggested that surface structural relaxation is promoted by an immeasurably small quantity of molecular water diffusing much more deeply than the hydroxyl diffusion front [4]. If the structural relaxation kinetics is governed by the glass viscosity [10], the kinetics should be independent of the specimen size or shape. On the other hand, if the surface structural relaxation kinetics is governed by a diffusion process, the effect of specimen size and shape should appear.

Prediction of properties after a heat treatment is important for many glass products, such as optical waveguides, display substrates, and micro-lenses. Sizes of these products are sometimes quite small: for example, the diameter of commercial optical fiber is typically  $\sim 100 \mu\text{m}$ . If structural relaxation shows a size effect, prediction of properties after a heat-treatment should be influenced by the specimen size. In this study, the effect of specimen size and shape on surface structural relaxation kinetics in silica glass was examined.

## 2. Experimental procedure

Fiber and plate samples of a silica glass with the same composition were used in this study. The fiber samples were commercial single mode optical fibers made by Furukawa Electric Co. in Tokyo, Japan using the chemical vapor deposition method. The fibers consist of  $\text{GeO}_2\text{-SiO}_2$  core with a diameter of 10  $\mu\text{m}$  surrounded by pure  $\text{SiO}_2$  cladding with an outside diameter of 125  $\mu\text{m}$ . The presence of the core glass with much smaller diameter does not seem to have any influence on the structural relaxation of the fiber cladding. In fact, Saito et al. showed that the bulk structural relaxation time of a cladding glass of optical fiber was independent of compositions of various core glasses [11]. This cladding glass contains chlorine at approximately 1000 ppm in weight and a negligible amount of OH, below 0.1 ppm. This amount of chlorine is usually contained in silica glasses for optical fibers and is known to reduce the glass viscosity to some extent as was reported earlier [2]. The commercial fibers were soaked in hot sulfuric acid–nitric acid (98%  $\text{H}_2\text{SO}_4$ –2%  $\text{HNO}_3$ ) solution at 200 °C for 30 s in order to remove the plastic coating, and then cut to approximately 3 cm in length. The plate samples were prepared from a preform for the cladding

glass of the fiber. The preform was cut to approximately 10 mm  $\times$  10 mm  $\times$  2 mm, using a low-speed saw equipped with a diamond blade. The plate samples were then polished with a series of SiC papers with decreasing grain sizes starting with 240 grit paper and ending with 0.06  $\mu\text{m}$  cerium oxide slurry to obtain an optically smooth finish. Both the fiber sample and the plate sample were heat-treated at 1200 °C for 6 h in dry air to establish the metastable equilibrium state and then air quenched. Fictive temperatures of the samples are expected to be same as the heat-treatment temperature of 1200 °C.

The samples were then heated at 950 °C in 355 Torr water vapor pressure to determine the surface structural relaxation kinetics. The water vapor was created by passing air through a hot water bath kept at 80 °C. During the heat-treatment, samples were periodically removed from the furnace and their IR reflection spectra were collected to determine their surface fictive temperature. The IR reflection spectra were obtained by using a Nicolet Fourier Transform Infrared (FTIR) spectrometer with a Spectra-Tech microscope attachment. The beam size employed for the fiber sample was 20  $\mu\text{m}$   $\times$  400  $\mu\text{m}$  rectangle with the longer dimension being parallel to fiber axis. For the plate sample a circular beam with 100  $\mu\text{m}$  in diameter was used. Earlier, a simple IR technique to determine the fictive temperature of silica glass was developed [12,13]. The IR peak position of silica structural band is known to correlate with the fictive temperature of silica glasses. For the measurement of the surface fictive temperature, the IR reflection of structural band at  $\sim 1120 \text{ cm}^{-1}$ , which is the asymmetric stretching vibration of the Si–O–Si band, can be used, and for bulk fictive temperature, the IR absorbance of an overtone peak at  $2260 \text{ cm}^{-1}$  can be used. The IR reflection of this  $\sim 1120 \text{ cm}^{-1}$  peak probes the fictive temperature of the surface layer of effective thickness  $\sim 0.22 \mu\text{m}$  [14].

Depending upon the atmosphere of the heat treatment, hydroxyl contents in the glass surface should be different

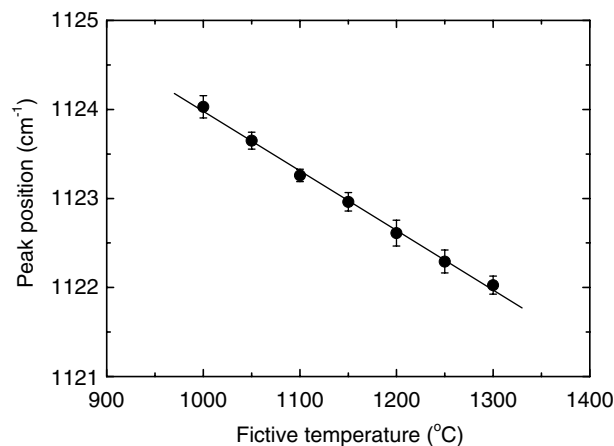


Fig. 1. IR reflection peak wavenumber vs. fictive temperature for silica glass optical fiber cladding. The straight line is linear regression fit to the data [12].

after the heat-treatment. However, the equilibrium value of the IR reflection peak wavenumber was the same at a constant heating temperature independent of the heat-treatment atmosphere within experimental error [13]. Thus, regardless of atmosphere, surface fictive temperature can be determined by the IR reflection peak wavenumber of the silica structural band. Fig. 1 shows the relationship between fictive temperature and the IR peak wavenumber around  $\sim 1120 \text{ cm}^{-1}$  of the silica glass surface determined earlier [12] by using the same method as in the present experiment. The straight line which is linear regression fit to the data can be expressed as,

$$\nu (\text{cm}^{-1}) = 1132.501 - 0.00669T_f(\text{K}) \quad (2)$$

with the wavenumber error range of  $\pm 0.10 \text{ cm}^{-1}$ . The measured IR peak wavenumber can be converted to the surface fictive temperature using this relation.

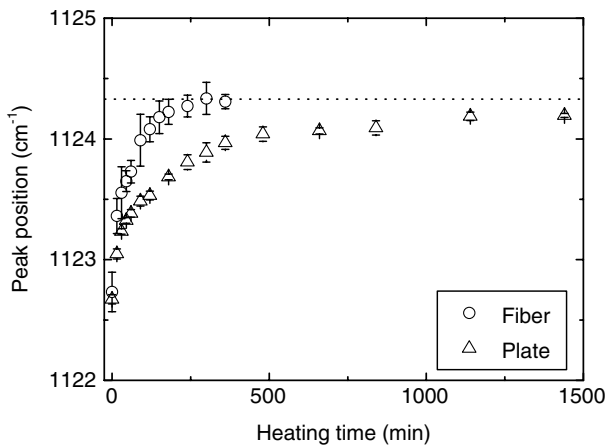


Fig. 2. The IR peak wavenumber variation with the heat-treatment time at  $950 \text{ }^\circ\text{C}$  in 355 Torr water vapor pressure for the silica glass fiber sample and the plate sample with the initial fictive temperature of  $1200 \text{ }^\circ\text{C}$ . The dotted horizontal line indicates the equilibrium value at  $950 \text{ }^\circ\text{C}$ .

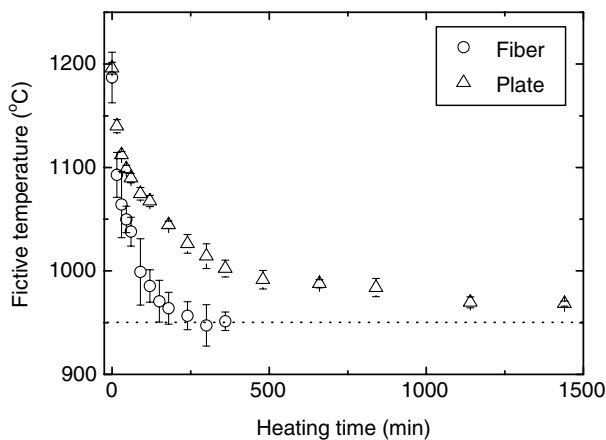


Fig. 3. Fictive temperature variation with the heat-treatment time at  $950 \text{ }^\circ\text{C}$  in 355 Torr water vapor pressure for the silica glass fiber sample and plate sample. The dotted horizontal line indicates the final equilibrium value.

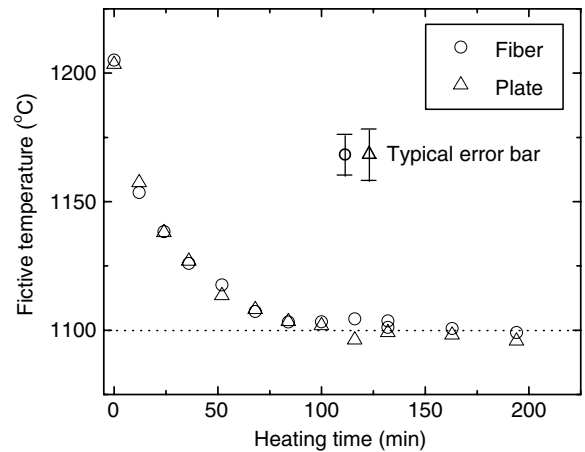


Fig. 4. Bulk fictive temperature variation with the heat-treatment at  $1100 \text{ }^\circ\text{C}$  in dry atmosphere for silica glass fiber and plate samples with the initial fictive temperature of  $1200 \text{ }^\circ\text{C}$ . The dotted horizontal line indicates the final equilibrium value [15].

### 3. Results

The change of IR peak wavenumber of the fiber sample and the plate sample with the heat-treatment time at  $950 \text{ }^\circ\text{C}$  in 355 Torr water vapor is shown in Fig. 2. Fig. 3 shows the corresponding changes of fictive temperature calculated from the IR peak wavenumber using the Eq. (2). The surface structural relaxation of the plate sample was slower than that of the fiber, even though the glass composition and the initial fictive temperature were the same. This result indicates that surface structural relaxation kinetics depends upon the specimen size and shape.

Fig. 4 shows, for comparison, the bulk structural relaxation data for the same glass samples obtained earlier [15]. These data were obtained by measuring the IR absorption peak shift and comparing the results with the calibration curves of the IR peak wavenumber and the fictive temperature. For the bulk relaxation study of the plate sample, the absorption peak at  $2260 \text{ cm}^{-1}$  was used, while for the bulk relaxation of the fiber sample, the absorption peak at  $1800 \text{ cm}^{-1}$  was used [15]. It can be seen that both fiber and plate samples exhibit the same bulk structural relaxation characteristics within experimental error in a dry atmosphere.

### 4. Discussion

In earlier studies, it was shown that the surface structural relaxation propagates into the glass as a diffusion process [9]. Thus, the solutions of the diffusion equation used for various diffusing species into a solid [16] can be used with the understanding that the concentration of the diffusing species corresponds to the extent of the surface structural relaxation.

The effective diffusion coefficients,  $D$ , for surface structural relaxation have been determined by Davis [17] and Davis and Tomozawa [9] using thin films of thickness  $\sim 100 \text{ }\mu\text{m}$  of various silica glasses as a function of

temperature under 355 Torr of water vapor, the same water vapor pressure used in the present experiment. In their method, they measured the time dependence of structural relaxation of the thin films by the IR absorbance and obtained the diffusion coefficient by comparing the data with the equation for diffusion uptake,  $M$ , given by

$$\frac{M}{M_\infty} = 1 - \sum_{n=0}^{\infty} \frac{8}{(2n+1)^2 \pi^2} \exp\left(-D \frac{(2n+1)^2 \pi^2 t}{4l^2}\right) \quad (3)$$

where  $M_\infty$  is the equilibrium value of the total amount of uptake and  $l$  is the half thickness of the plate [16].

Agarwal [18] and Agarwal and Tomozawa [2] also determined the diffusion coefficient for surface structural relaxation for Furukawa silica glass, the same glass used in the present experiment. They also used the relaxation kinetics study of thin silica films by IR absorption to obtain the diffusion coefficient of surface relaxation [18]. With this glass at a high temperature, because of its lower viscosity compared with other silica glasses, bulk structural relaxation was superimposed on the surface structural relaxation and they separated these two contributions by measuring the relaxation kinetics of the silica glass film samples of different thicknesses. Agarwal [18] also obtained the diffusion coefficient of surface structural relaxation of the glass by measuring the relaxation depth profile of thick samples by IR reflection combined with successive etching and comparing the diffusion profile with the complementary error function. Two different methods gave consistent values of the diffusion coefficient for surface structural relaxation.

All the previously obtained diffusion coefficients of the surface structural relaxation for various silica glasses are summarized in Fig. 5. These diffusion coefficients were obtained by comparing the surface structural relaxation data with the diffusion equations solved under the assumption

of the constant surface concentration. The logarithm of the diffusion coefficients obtained in this manner for Furukawa silica glass [18], the same glass used in the present experiment, can be represented by a straight line when plotted against the reciprocal absolute temperature, as shown in Fig. 5. The activation energy for the diffusion coefficient was found to be  $270 \pm 16$  kJ/mol.

The present data shown in Fig. 3 clearly indicate that the surface concentration or the surface extent of the relaxation is time-dependent. Therefore, the boundary condition of the constant surface concentration employed earlier is not strictly valid. Here, it will be determined, first, how much error is introduced into the estimated diffusion coefficient assuming a constant surface concentration. At  $950^\circ\text{C}$ , the heat-treatment temperature employed in the present experiment, the diffusion coefficient of the surface structural relaxation is approximately  $10^{-9}$  cm<sup>2</sup>/s. The shortest heat-treatment time employed was 15 minutes. The corresponding diffusion distance of the surface structural relaxation is estimated as  $\sqrt{Dt} \approx 10$   $\mu\text{m}$ . Thus, even in the shortest heat-treatment time, the diffusion distance is far greater than the effective distance the IR reflection beam probes, 0.22  $\mu\text{m}$ . The structural relaxation at the effective depth of the probe, 0.22  $\mu\text{m}$ , therefore, is expected to be same as the relaxation at the surface. Therefore, the measured data by IR reflection can be regarded as representing the extent of the relaxation at the surface or the surface concentration.

The most popular time-dependent surface concentration boundary condition is given by

$$J(0, t) = \alpha(C_0 - C_s) \quad (4)$$

where  $\alpha$  is the proportionality constant between the diffusate flux,  $J$ , at the specimen surface and the difference in actual concentration at the specimen surface,  $C_s$ , and equilibrium concentration of the sample,  $C_0$ .

By using this boundary condition, the concentration in a semi-infinite sample at the depth  $x$  from the surface at time  $t$  can be expressed by [16]

$$\frac{C}{C_0} = \operatorname{erfc} \frac{x}{2\sqrt{Dt}} - \exp\left(\frac{\alpha}{D}x + \frac{\alpha^2 Dt}{D^2}\right) \operatorname{erfc} \left\{ \frac{x}{2\sqrt{Dt}} + \frac{\alpha\sqrt{Dt}}{D} \right\} \quad (5)$$

The surface concentration at time  $t$ ,  $C_s$ , can be expressed by

$$\frac{C_s}{C_0} = 1 - \exp\left(\frac{\alpha^2}{D}t\right) \operatorname{erfc} \left( \sqrt{\frac{\alpha^2}{D}t} \right) \quad (6)$$

From this equation, it is clear that the surface concentration is a function of the parameter,  $\alpha^2/D$ . The surface relaxation data for the plate sample was compared with the Eq. (6) with various values of  $\alpha^2/D$ , as shown in Fig. 6(a). The value of  $\alpha^2/D = 0.00012$  s shown in a solid line, appears to fit the data best. The previous experiment using the same glass [2] showed much faster surface relaxation than that of bulk and the bulk relaxation was negligible under the condition at  $1000^\circ\text{C}$  for 1.5 h under the same atmosphere.

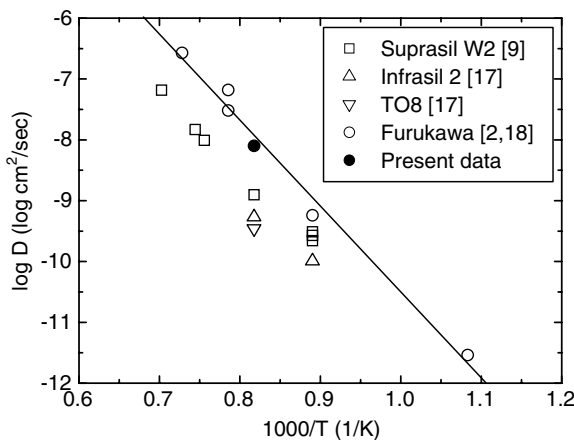


Fig. 5. Effective diffusion coefficient of surface structural relaxation for various silica glasses, obtained by previous works. Suparsil W2 [9], Infrasil 2 [17], TO8 [17], Furukawa glass [2,18]. The filled circle indicates the diffusion coefficient used in the present analysis. The straight line is linear regression fit to the data for Furukawa glass ( $\circ$  and  $\bullet$ ) with correlation coefficient of 0.986. The estimated activation energy for the effective diffusion coefficient of the surface structural relaxation is  $270 \pm 16$  kJ/mol.

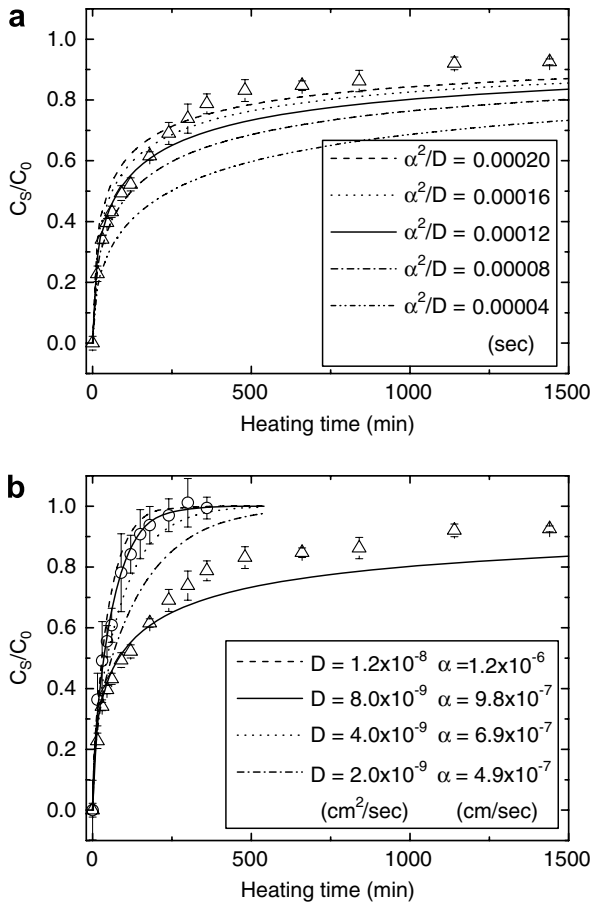


Fig. 6. (a) Structural relaxation kinetics of the surface of Furukawa silica glass compared with the time-dependent surface concentration for diffusion in semi-infinite samples. Various different values of  $\alpha^2/D$  were used to obtain the best fit shown as the solid line. (b) For the chosen  $\alpha^2/D = 0.00012$  s, various values of  $D$  and  $\alpha$  were used to obtain the best fit shown as the solid line for the fiber data (○) using the diffusion equation for the cylindrical sample. The data (Δ) for the plate sample are also shown.

However, in the case of a longer heat-treatment time at this temperature for this glass, some contribution from the bulk relaxation is expected and may be the cause of the observed discrepancy between the data and the simulation.

The concentration in a cylinder with radius  $a$ , at the distance  $r$  from the center, under the same time-dependent surface concentration boundary condition, Eq. (4), can be expressed by [16]

$$\frac{C}{C_0} = 1 - \sum_{n=1}^{\infty} \frac{2(\alpha x/D) J_0(r\beta_n/a)}{\{\beta_n^2 + (\alpha x/D)^2\} J_0(\beta_n)} \exp(-\beta_n^2 Dt/a^2), \quad (7)$$

where  $\beta_n$ s represent the roots of

$$\beta J_1(\beta) - (\alpha x/D) J_0(\beta) = 0, \quad (8)$$

where  $J_n$ s represent Bessel functions. The surface concentration on the cylinder surface at time  $t$  can be expressed by

$$\frac{C_s}{C_0} = 1 - \sum_{n=1}^{\infty} \frac{2(\alpha x/D)}{\beta_n^2 + (\alpha x/D)^2} \exp(-\beta_n^2 Dt/a^2). \quad (9)$$

The surface relaxation data for the silica fiber were compared with this Eq. (9) using various diffusion coefficients near the value reported by Agarwal [18] as shown in Fig. 6(b). In this figure, all the chosen parameters correspond to  $\alpha^2/D = 0.00012$  s, which was found above to fit the semi-infinite plate data best. The summation in Eq. (9) was used up to  $n = 6$ , using the values of  $\beta_n$ s listed in Ref. [16]. In Fig. 6(b), the data for the plates sample are also shown for comparison. This analysis shows that the best fit, given by the solid line, is obtained when  $D = 8.0 \times 10^{-9}$  cm<sup>2</sup>/s and  $\alpha = 9.8 \times 10^{-7}$  cm/s are used. These values will be used for all the subsequent analysis. The estimated diffusion coefficient is shown in Fig. 5 as the filled circle, and is found close to those estimated using the boundary condition of a constant surface concentration. Apparently, the diffusion coefficient estimated is not affected greatly by the chosen boundary conditions.

The Eq. (9) indicates the surface relaxation kinetics is a function of the fiber radius,  $a$ , also. In Fig. 7, the surface relaxation of the silica fibers with various radii are compared at 950 °C and under 355 Torr water vapor using same  $\alpha$  and  $D$  values. It is clear that fibers with smaller diameters relax faster.

The size effect on the surface relaxation is expected for other geometries than fibers, also. Under the same boundary condition, the concentration profile at the depth  $x$  from the center of the thin plate with thickness,  $2l$ , can be expressed as [16]

$$\frac{C}{C_0} = 1 - \sum_{n=1}^{\infty} \frac{2(l\alpha/D) \cos(\beta_n x/l)}{\{\beta_n^2 + (l\alpha/D)^2 + (l\alpha/D)\} \cos \beta_n} \times \exp(-\beta_n^2 Dt/l^2), \quad (10)$$

where  $\beta_n$ s are the roots of

$$\beta \tan \beta - (l\alpha/D) = 0. \quad (11)$$

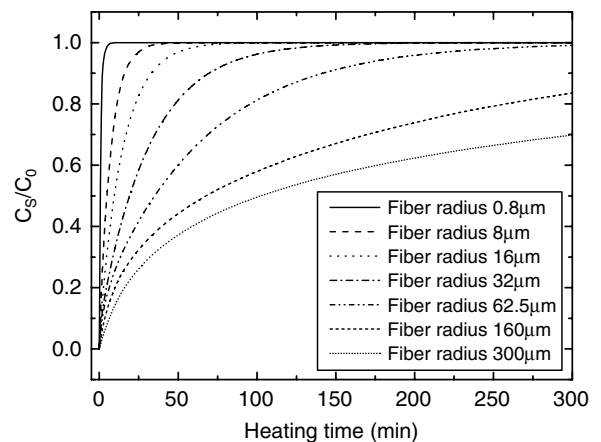


Fig. 7. Time variation of the extent of surface structural relaxation of small fibers normalized by the final value during the heat-treatment time at 950 °C in 355 Torr water vapor pressure simulated by Eq. (9).

The concentration at the surface of the thin plate at time  $t$  can be expressed by

$$\frac{C_s}{C_0} = 1 - \sum_{n=1}^{\infty} \frac{2(l\alpha/D)}{\beta_n^2 + (l\alpha/D)^2 + (l\alpha/D)} \exp(-\beta_n^2 Dt/l^2). \quad (12)$$

By using this equation, the surface structural relaxations of thin plates with various thicknesses are shown in Fig. 8. In this figure also, the summation in Eq. (12) was made up to  $n = 6$ .

In the case of small spheres, with radius  $a$ , the concentration at the distance  $r$  from the center can be expressed as [16]

$$\frac{C}{C_0} = \frac{2a^2\alpha}{rD} \sum_{n=1}^{\infty} \frac{\exp(-\beta_n^2 Dt/a^2)}{\{\beta_n^2 + (a\alpha/D)^2 - (a\alpha/D)\}} \frac{\sin \beta_n r/a}{\sin \beta_n}, \quad (13)$$

where  $\beta_n$ s are the roots of

$$\beta \cot \beta + (a\alpha/D) - 1 = 0. \quad (14)$$

The surface concentration on the small sphere at time  $t$  can be expressed by

$$\frac{C_s}{C_0} = \frac{2a\alpha}{D} \sum_{n=1}^{\infty} \frac{1}{\beta_n^2 + (a\alpha/D)^2 - (a\alpha/D)} \exp(-\beta_n^2 Dt/a^2) \quad (15)$$

The expected surface structural relaxations of small spheres with various radii are shown in Fig. 9. The summation in Eq. (15) was made up to  $n = 6$ . These equations for diffusion profiles and surface concentrations for specimens with smaller dimensions become the same as those for semi-infinite plates, Eqs. (5) and (6), as they should, when the size of the specimen becomes large since the same boundary condition is used for all the equations.

In order to evaluate the degree of speeding up of the surface structural relaxation for smaller samples, the apparent structural relaxation time was evaluated. Qualitatively,

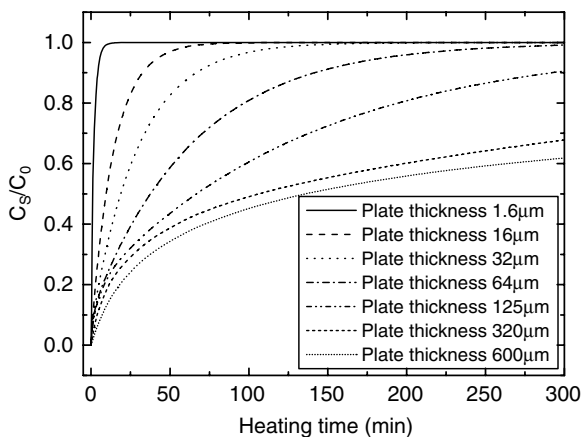


Fig. 8. Time variation of the extent of surface structural relaxation of thin plates normalized by the final value during the heat-treatment time at 950 °C in 355 Torr water vapor pressure simulated by Eq. (12).

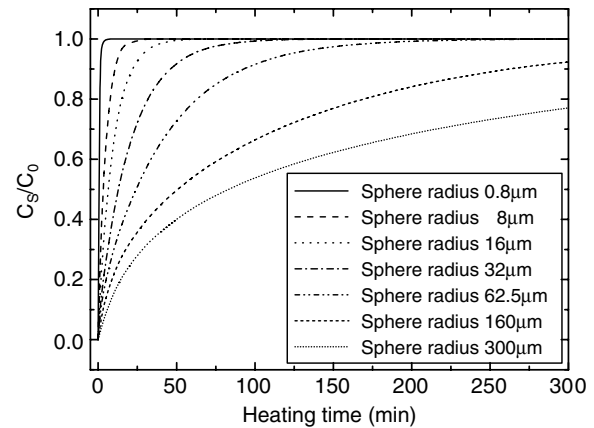


Fig. 9. Time variation of the extent of the surface structural relaxation of small spheres normalized by the final value during the heat-treatment time at 950 °C in 355 Torr water vapor pressure simulated by Eq. (15).

Eqs. (9), (12) and (15) indicate the reduction of the relaxation time with decrease of the sample size. If the first term of the summation in these equations dominates compared with the subsequent terms, the surface structural relaxation time is expected to scale with the square of the dimension, i.e.,  $a^2$  or  $l^2$ . In reality, the subsequent terms cannot be ignored. For quantitative analysis, the surface concentration variations shown in Figs. 7–9 were fitted with the following Kohlrausch–Williams–Watts (KWW) function, which is also known as the stretched exponential function [19].

$$\frac{C_s}{C_0} = 1 - \exp\left[-\left(\frac{t}{\tau}\right)^{\beta_{\text{KWW}}}\right]. \quad (16)$$

First, the relaxation parameters,  $\tau$  and  $\beta_{\text{KWW}}$ , were obtained for the experimental data represented by the solid lines shown in Fig. 6(b). The observed deviation of the experimental data for the plate sample from the simulation is probably due to the contribution of bulk relaxation [2] as pointed out earlier. The obtained parameters,  $\tau$  and  $\beta_{\text{KWW}}$ , were 53 min and 0.76 for fiber, and 183 min and 0.51 for plate, respectively. The apparent surface structural relaxation times for specimens with different dimensions were obtained in the similar manner using the simulation shown in Figs. 7–9. The estimated relaxation times,  $\tau$ , for samples with smaller dimensions were normalized by the relaxation time,  $\tau_{\infty}$ , of the surface relaxation time of a semi-infinite sample and are plotted in Fig. 10 as a function of the specimen radius  $a$  or half thickness  $l$ . The relaxation time for the silica fiber obtained in the present experiment is also included in the figure and can be seen to agree with the simulation result. This figure indicates that relaxation time decreases as the specimen size decreases and that surface structural relaxation time depends on the sample shape as well as size. In the case of small particle, fiber or thin film of  $\sim 1 \mu\text{m}$  dimension, the surface structural relaxation time is expected to be smaller than a large sample by more than two orders of magnitude at 950 °C under 355 Torr of water vapor.

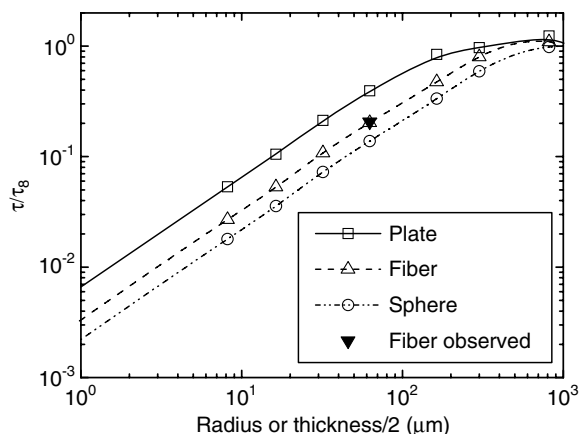


Fig. 10. Specimen size dependency of the surface structural relaxation time which is normalized by the surface structural relaxation time of a large bulk sample. ▼ marks the experimental data for optical fiber cladding. The error for the plot is smaller than the symbol size. Lines are guides to the eyes.

## 5. Conclusions

The surface structural relaxation of the silica glass fiber was faster than that of the silica glass plate, even though the glass composition and the initial fictive temperature of both samples were the same. The observed different surface structural relaxation kinetics of the plate and fiber can be simulated using diffusion equations with time-dependent surface concentration. This result indicates that surface relaxation shows a general size effect. The changes of the surface structural relaxation times for various shapes and sizes of silica glass samples at a constant temperature were estimated using diffusion equations with the same boundary condition. The results indicate that the surface structural relaxation of micrometer sized particles, fibers, and thin films should be faster than that of the bulk sample with the same composition by at least two orders of magnitude.

## Acknowledgement

The work was supported by NSF grant DMR-0352773. The glass samples used in the present research were provided by Furukawa Electric Co., in Tokyo, Japan. The authors benefited from the discussion with Dr S.-R Ryu of Rensselaer Polytechnic Institute.

## References

- [1] A.Q. Tool, *J. Am. Ceram. Soc.* 29 (1946) 240.
- [2] A. Agarwal, M. Tomozawa, *J. Non-Cryst. Solids* 209 (1997) 264.
- [3] Y.-L. Peng, M. Tomozawa, T.A. Blanchet, *J. Non-Cryst. Solids* 222 (1997) 376.
- [4] M. Tomozawa, D.-L. Kim, A. Agrarwal, K.M. Davis, *J. Non-Cryst. Solids* 288 (2001) 73.
- [5] R.H. Doremus, in: J.W. Mitchell, R.C. DeVries, R.W. Roberts, P. Cannon (Eds.), *Reactivity of Solids*, Wiley, New York, 1969, p. 667.
- [6] K.M. Davis, M. Tomozawa, *J. Non-Cryst. Solids* 201 (1996) 177.
- [7] M. Nowak, H. Behrens, *Geochim. Cosmochim. Acta* 59 (1969) 3445.
- [8] A. Shen, H. Keppler, *Am. Mineral.* 80 (1995) 1335.
- [9] K.M. Davis, M. Tomozawa, *J. Non-Cryst. Solids* 185 (1995) 203.
- [10] G.W. Scherer, *Relaxation in Glass and Composites*, Wiley, New York, 1986.
- [11] K. Saito, M. Yamaguchi, A.J. Ikushima, K. Ohsono, Y. Kurosawa, *J. Appl. Phys.* 95 (2004) 1733.
- [12] D.-L. Kim, M. Tomozawa, *J. Non-Cryst. Solids* 286 (2001) 132.
- [13] A. Agrarwal, K.M. Davis, M. Tomozawa, *J. Non-Cryst. Solids* 185 (1995) 191.
- [14] M. Tomozawa, R.W. Hepburn, *J. Non-Cryst. Solids* 345 & 346 (2004) 449.
- [15] S.-R Ryu, PhD thesis, Rensselaer Polytechnic Institute, Troy, NY, 2005.
- [16] J. Crank, *The Mathematics of Diffusion*, Oxford, New York, 1975.
- [17] K.M. Davis, PhD thesis, Rensselaer Polytechnic Institute, Troy, NY, 1994.
- [18] A. Agarwal, PhD thesis, Rensselaer Polytechnic Institute, Troy, NY, 1995.
- [19] S.M. Rekhson, O.V. Mazurin, *J. Am. Ceram. Soc.* 57 (1974) 327.